Are alpha Cygni Variables a Homogeneous Class?

Joyce A. Guzik[1]
Los Alamos National Laboratory
XTD-NTA, MS T-082, Los Alamos, NM 87545
joy@lanl.gov

Claire Whitley[1]*, Nova Moore*[1]*, James Kay*[2]*, Brian Kloppenborg*[3]*, Tom Calderwood*[3]*, Madeline Marshall*[1]*, Jason Jackiewicz*[4]

[1]Los Alamos National Laboratory
[2]University of Vermont
[3]American Association of Variable Star Observers
[4]New Mexico State University

Abstract

Alpha Cygni (ACYG) variables are luminous O-, B-, and A-type supergiants that show low-amplitude photometric variability on timescales of days to weeks. The AAVSO VSX database lists 185 ACYG variables, but the physical causes of their variability and their evolutionary states are not well established. While recently we have focused on the prototype alpha Cygni (Deneb), here we begin to examine photometric data sets for other ACYG stars, including TESS light curves, 8.6-year light curves extracted from Solar Mass Ejection Imager (SMEI) data, MOST and BRITE photometry for Rigel, and recent AAVSO Photoelectric Photometry observations. SMEI light curves were processed for 33 of the 185 cataloged ACYG variables bright enough for useful analysis. Periodograms from the full SMEI light curves usually show many significant low-frequency peaks. Examination of the light curve for Rigel shows transitions between larger amplitude, longer-period variability and intervals of lower amplitude oscillations or less coherent behavior. The excellent agreement between contemporaneous MOST and SMEI photometry for Rigel helps to validate the SMEI reductions. We identify two promising candidate gravity-mode/Rossby-mode pulsators: TIC 179508685, using 36 sectors of TESS data, and 19 Cep, using the 8.6-year SMEI data set. These investigations show that ACYG variables are likely not a homogeneous class in a physical sense. However, it is premature to sort them into subclasses by variability mechanism.

1. Introduction

The alpha Cygni (ACYG) variables are spectral type O, B, and A supergiants which show photometric variability of around 0.1 magnitudes (e.g., van Genderen et al. 1989; Richardson et al. 2011). The light curves for the prototype Deneb sometimes show a quasi-periodicity of around 12 days which damps out after a few cycles. (see, e.g., Abt et al. 2023, Guzik et al. 2024a, 2024b, 2025).

The AAVSO International Variable Star Index (VSX, Watson et al. 2006) lists 185 ACYG variables. The VSX ACYG description states that the light curves "often seem irregular, being caused by the superposition of many oscillations with close periods. Cycles from several days to several weeks are observed." However, there is no consensus in the literature that these variables are pulsating in multiple modes, on the type of oscillation (e.g., p-mode, g-mode, 'strange' modes), or the mechanism causing the variability. Phenomena such as stellar winds, subsurface convection, shocks, binarity/multiplicity, and magnetic fields may influence the variability. There is also no consensus on the evolutionary state of these stars, whether they are on their first crossing of the Hertzsprung-Russell diagram to the red after exhausting core hydrogen, or are on their way back toward the blue, perhaps undergoing core helium burning.

In recent talks and proceedings for SAS and AAVSO meetings (Guzik et al. 2024a, 2024b, 2025), we have focused on observations of Deneb. We have begun to examine the behavior of other bright ACYG variables (Guzik et al. 2026), using 27-day light curves from the NASA TESS spacecraft, and are now reviewing the 8.6-year-long data set for bright stars from the Solar Mass Ejection Imager (SMEI). We highlight results from a few light curves, characterizing the diversity and similarity of behavior of members of this class, and possible significant periodicities uncovered. We also take a closer look at the ACYG star Rigel, reviewing conclusions based on photometric data from the Canadian MOST satellite and ground-based radial velocity measurements, and previewing data from TESS, SMEI, the BRITE Constellation, and the AAVSO Photoelectric Photometry (PEP) observing team.

We comment on the location of the ACYG variables near other classes of pulsating variable stars in the H-R Diagram (e.g., beta Cep, LBV, SLF, and RV Tauri variables) and on whether they may have physical properties in common with these classes.

2. TESS Observations

Because ACYG stars in general do not have strictly periodic variations, sparse data points cannot be phased to reconstruct a light curve as is possible with classical variables such as Cepheids. Their small amplitudes make them challenging to monitor from the ground, and ideally at least one data point per night with uncertainty around 0.01 magnitudes is needed to accurately characterize their behavior.

One ongoing opportunity for continuous time series observation is available using the Transiting Exoplanet Survey Satellite (TESS, Ricker et al. 2015). TESS was launched April 18, 2018 into a 13.7-day lunar resonance orbit. Its four 2048 x 2048 pixel CCD cameras with 21 arc seconds per pixel observe strips of the sky called 'sectors' for 27 days, before transitioning to the next sector. The observing cadence during the first two years of operation was 30 minutes; the cadence was reduced to 10 minutes for years 3-4, and 3.3 minutes for subsequent years. TESS's main mission is to search for planets around nearby, mostly M-dwarf, stars and has revealed 892 confirmed planets and 7931 candidates as of May 2026 (https://exoplanetarchive.ipac.caltech.edu/).

Figures 1 and 2 show the TESS fields of view for Sectors 97-107 being observed September 2025-September 2026, and Sectors 108-121 planned for September 2026-September 2027. Some of the fields overlap, allowing the possibility for continuous observing for two or more 27-day consecutive sectors for stars that fall in these fields. While the cadence and precision for TESS observations are high, unfortunately TESS is still not ideal to fully characterize ACYG stars, which have periodicities longer than the time series length. Bright stars present a challenge for TESS with pixel saturation, requiring special techniques such as 'halo photometry' (e.g., Rudrasingam 2026) to create accurate light curves. Detrending pipelines must be used with caution since they often remove the long-period signals characteristic of ACYG variations. Methods to stitch together variations between cameras and sectors to put flux levels on an absolute scale are subject of active research.

Of the 185 ACYG stars in the VSX catalog, 75 of them fall on the TESS field of view during Cycle 8, and 74 will fall in the TESS field of view during Cycle 9, with 32 stars in common for both sectors. These stars range from TESS magnitudes 0.706 (Rigel) to 12.62. We proposed to TESS General Investigator program to observe these stars, and their light curves will be processed from the full-frame images by TESS headquarters and will be publicly available at the Mikulski Archive for Space Telescopes (MAST, https://archive.stsci.edu/).

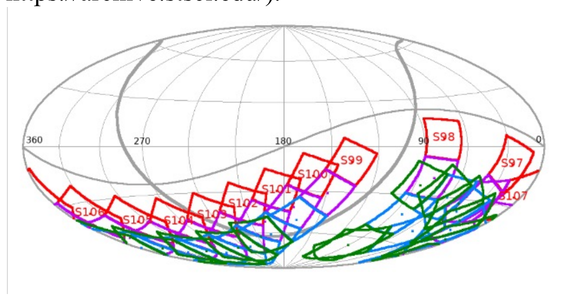

Figure 1: TESS fields of view for Cycle 8, Sectors 97-107, Sept. 2025-2026 (Equatorial coordinate view).

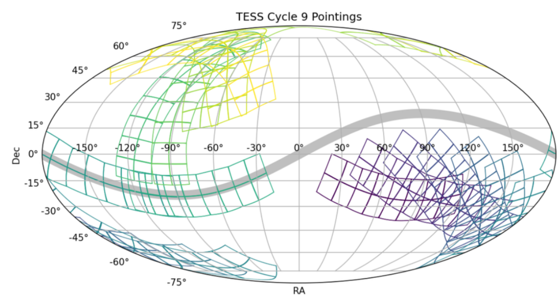

Figure 2: TESS fields of view for Cycle 9, Sectors 108-121, Sept. 2026-Sept. 2027 (Equatorial coordinate view).

For the 75 ACYG stars to be observed during Cycle 8, we attempted to place the stars approximately on a Hertzsprung-Russell (H-R) diagram (Figure 3) to see their location compared to known variable star types. Many of the stars were too bright to obtain Gaia DR3 (Gaia Collaboration 2023) parallaxes. We used SIMBAD (https://simbad.u-strasbg.fr/simbad/) and the TESS Input Catalog (Stassun et al. 2019) to find values for effective temperatures, distances and visual magnitudes, and approximated bolometric corrections using the table from *Allen's Astrophysical Quantities* (2000). We did not correct for interstellar reddening. Enough information was available to place the stars on the H-R diagram for only about 50 stars. The ACYG stars appear to be located throughout the upper part of the H-R diagram, close to the beta Cep (e.g., Stankov and Handler 2005), LBV (Humphreys and Davidson 1994), RV Tauri (Bódi and Kiss 2019), and SLF (Pedersen and Bildsten 2025) variables, and some may therefore be expected to have properties in common with these other variable star classes.

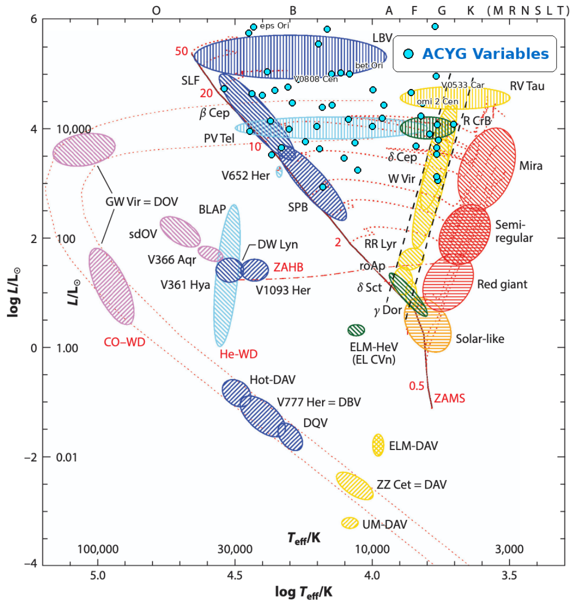

Figure 3: Pulsating variable star Hertzsprung-Russell diagram adapted from Jeffery et al. (2025) with approximate location of around 50 ACYG variables overlaid (blue circles).

All 75 of the stars observable during Cycle 8 have been observed in earlier TESS Sectors. For the 114th AAVSO meeting we reported on using the online TESS Extractor (Serna et al. 2021; Brasseur et al. 2019) tool to generate light curves from the TESS full-frame images and screened these for follow-up analysis and observations (Guzik et al. 2026). Figure 4 shows the detrended TESS Extractor light curve for Sectors 68-69 for one interesting star, TIC 179508685 (TESS mag 10.63, spectral type OB) which has 36 sectors (nearly three years) of TESS observations because of its proximity to the south ecliptic pole. One can see a short period of about 1.6 days, and a longer periodic trend of around 10 days that is removed by some pipelines.

We calculated a periodogram for this star combining light curve data from all 36 Sectors (Figure 5). The 1.66 -day period has the highest amplitude and is most likely a rotational frequency or a binary orbital frequency. Prewhitening of this data revealed more than 100 frequencies with signal to noise greater than 5. There are two clumps of peaks with significant power around 9 days and 17 days, and there is some regularity to the period spacings. Such a periodogram is typical of stars such as gamma Doradus or SPB (slowly pulsating B) stars pulsating in many nonradial gravity modes and/or Rossby modes (e.g., Saio et al. 2018, Li et al. 2020); combined with stellar modeling it is possible to identify the modes and use the period spacings to extract information such as surface and core rotation rates.

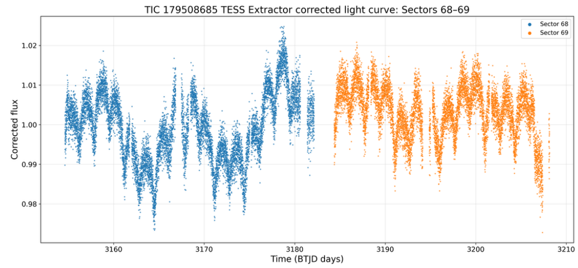

Figure 4: TESS Extractor detrended light curve for TIC 179508685, Sectors 68-69.

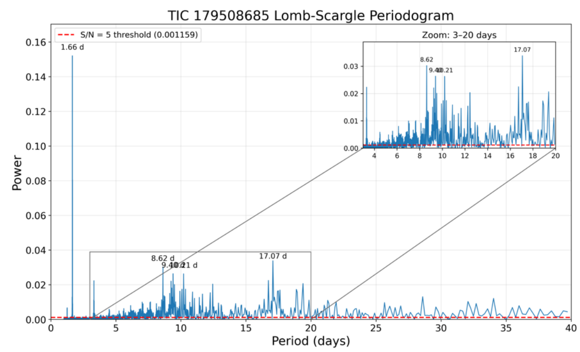

Figure 5: Lomb-Scargle Periodogram for TIC 179508685 using TESS Extractor light curve for 36 Sectors of TESS data.

3. SMEI Observations

At previous AAVSO and SAS meetings we reported on a first look at Deneb data taken by the Solar Mass Ejection Imager (SMEI, Jackson et al. 2004; Clover et al. 2011) during 8.6 years between 2003 and 2011. While intended to monitor solar activity, SMEI also imaged the sky and useful data were obtained for nearly all bright stars with V magnitude less than around 6. The SMEI cadence was one data point per Earth orbit, every 102 minutes (1.7 hours). These data had been stored on a hard drive by AAVSO Director Brian Kloppenborg but not yet processed for variable star research. Enlisting the help of AAVSO member James Kay, a pipeline has been developed to detrend and align the data from three SMEI cameras and to remove some artifacts. This pipeline was applied to 33 of the ACYG variables of the 185 listed in the VSX catalog which were bright enough to yield useful SMEI light curves.

Figure 6 illustrates three stages of processing steps for the SMEI Rigel data. These results are preliminary since more work needs to be done to remove remaining artifacts. We show a few highlights of findings for several ACYG stars based on the SMEI data.

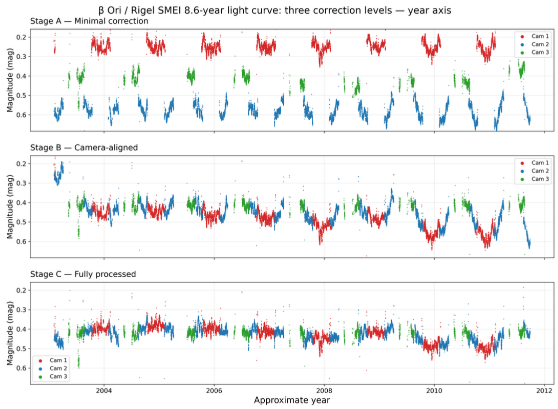

Figure 6: SMEI Rigel light curves after three stages of processing from pipeline created by James Kay and Brian Kloppenborg.

3.1 SMEI Deneb Data

Figure 7 shows the Lomb-Scargle periodogram for the 8.6 years of 'fully processed' SMEI data for alpha Cyg (Deneb). Deneb has V magnitude 1.25, and spectral type A2Ia. In these periodograms, FAP is an abbreviation for 'False Alarm Probability'. The peaks above FAP of 1% are considered credible periodicities in the data.

Although we have found from prior analyses of Deneb light and radial velocity data that Deneb shows a 12-day quasi-periodicity, this periodicity is too intermittent or irregular to show up in the periodogram for the full SMEI light curve.

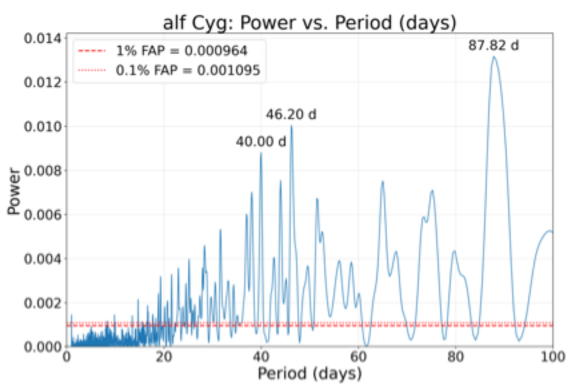

Figure 7: Lomb-Scargle periodogram generated from 8.6-year SMEI light curve for alpha Cygni (Deneb).

3.2 19 Cep

Figure 8 shows the periodogram from SMEI data for the ACYG star 19 Cep = HD 209975, with V magnitude 5.11 and spectral type O9Ib. As was the case for TIC 179508685, this periodogram shows characteristic clumps of modes with nearly equally spaced periods characteristic of gravity-mode and/or Rossby mode pulsations and is another excellent candidate for detailed asteroseismic studies. Figure 9 zooms in on the shorter period region where the period spacings can be seen clearly.

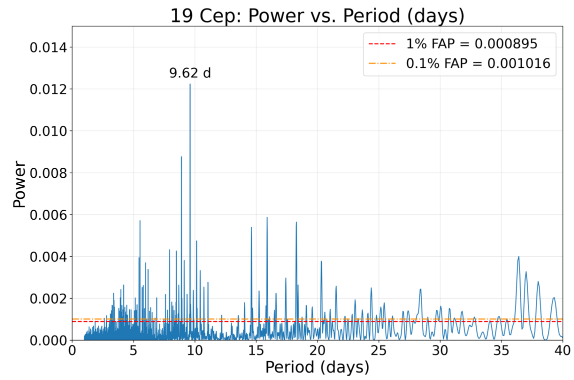

Figure 8: Lomb-Scargle periodogram generated from 8.6-year SMEI light curve for 19 Cep.

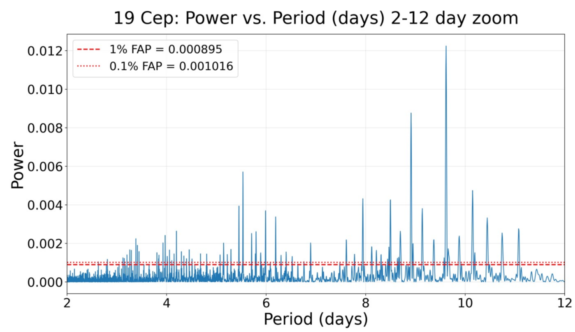

Figure 9: Zoom-in on 2 to 12-day portion of periodogram for 19 Cep.

3.3 eta CMa

Figure 10 shows the periodogram for eta CMa = HD 58350, with V magnitude 2.45 and spectral type B5Ia. This bright star is also known as Aludra and is located at the tip of the dog's tail in the Canis Major constellation. While the VSX database lists a characteristic period of 4.7 days for this star, there is only a small peak above the FAP threshold at this period, and instead more power at longer periods of around 35 and 52 days.

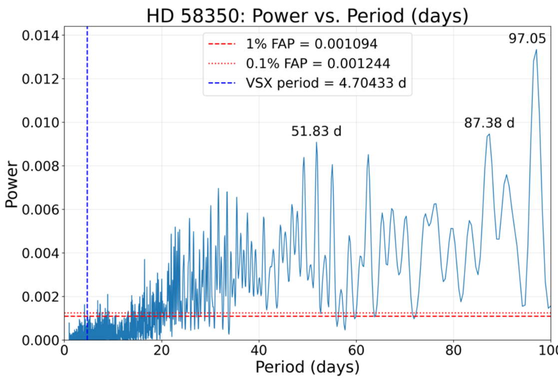

Figure 10: Lomb-Scargle periodogram generated from 8.6-year SMEI light curve for eta CMa.

3.4 sigma Cyg

Figure 11 shows the periodogram from the SMEI data for sigma Cyg = HD 202850, with V magnitude 4.24, and spectral type B9Iab. This ACYG star already has a full season of observational data taken by the AAVSO PEP observers in 2025, and observations will continue. The VSX catalog lists a very long 120-day periodicity, but shorter periods such as those with high power in the periodogram near 40 or 60 days might be detected by ground-based observers.

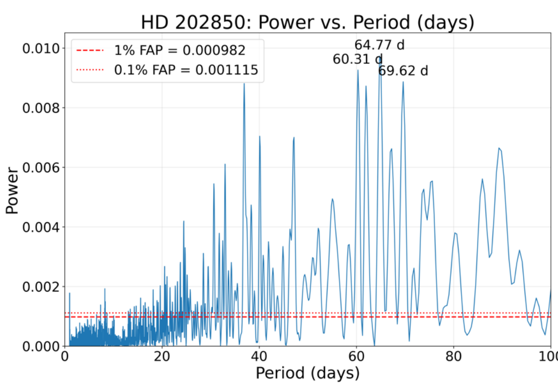

Figure 11: Lomb-Scargle periodogram generated from 8.6-year SMEI light curve for sigma Cyg.

3.5 V0566 Cas

Figure 12 shows the periodogram based on the SMEI data for V0566 Cas, also known as 6 Cas, HD 223385. This star has V magnitude 5.44-5.63 according to the VSX database and is a double or multiple star system according to the SIMBAD database, with stars of A2.5I and O9.8II spectral types. Abt et al. (2023) called attention to this star as having similarities to Deneb, namely spectral type and possibly age and evolutionary state.

For SMEI sigma Cyg data, the periodogram shows a significant peak at 36.50 days, very near to the periodicity reported in the VSX catalog of 37.26 days.

This star has been targeted by AAVSO PEP observers. AAVSO data is available at the AAVSO International Database (Kloppenborg 2023). Figure 13 shows 2024-2026 V-band data collected by observers Erwin van Bellegoij, David Brooks, Tom Calderwood, Brad Ferguson, Marcus Geselle, Paul Kneipp, and Pam Morgan-McKee. It will be interesting to see whether continued monitoring will confirm the 37-day periodicity, reveal other periodicities, and quantify consistency or discover more erratic behavior of this star.

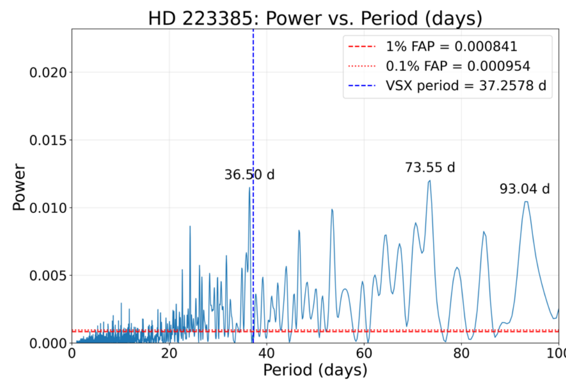

Figure 12: Lomb-Scargle periodogram generated from 8.6-year SMEI light curve for V0566 Cas.

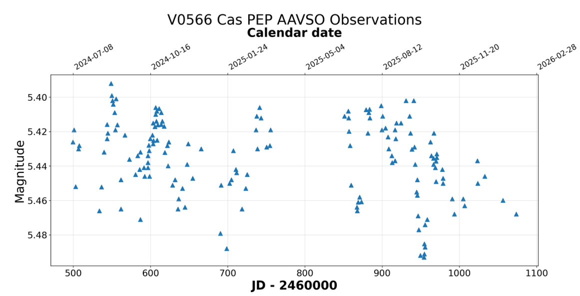

Figure 13: V-band AAVSO Photoelectric Photometry (PEP) observations of V0566 Cas for 2024-2026.

4. Closer Examination of Rigel Light Curves

We next take a closer look at the light curves for Rigel available from SMEI, the BRITE Constellation, the Canadian MOST satellite, and continuing ground-based observations by the PEP observing team. We do not discuss the TESS photometry for Rigel here, because extracting a light curve from TESS full-frame images for such a bright star requires special processing, and because TESS has observed Rigel for only a few 27-day sectors (5, 32, 98) so far.

4.1 Rigel SMEI Light Curve

We examined the entire 8.6 year SMEI light curve shown in Figure 6, zooming in on 50-day segments. We show four of these 59 segments to illustrate some typical and interesting behavior in the SMEI Rigel light curves. These plots all have the same y-axis scale to highlight relative amplitudes.

One notices in Figures 14, 16, and 17 that the light curve is showing low-amplitude short period oscillations punctuated by larger 0.03-0.05 mag variations with period around 5 days. At other times (e.g., Fig. 15 and 17), the light curve shows larger, up to 0.15 mag, variations with periodicities closer to 10 days. Sometimes the light curve shows properties of the transition between these two states. Note there are also artifacts in the light curves, e.g., two of them between days 2500 and 2510 in Fig. 16 that have not been removed. It will be worthwhile to quantify the frequency, duration, and coherency of behavior of these two states, toward reaching some interpretation.

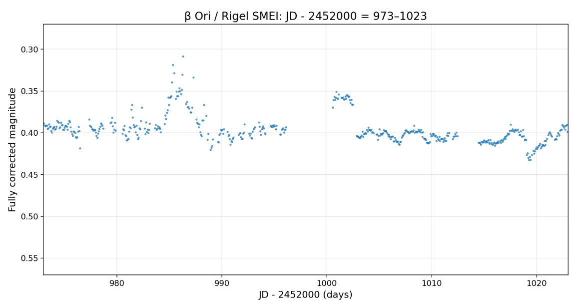

Figure 14: SMEI Rigel light curve for days 973-1023 after JD 2452000.

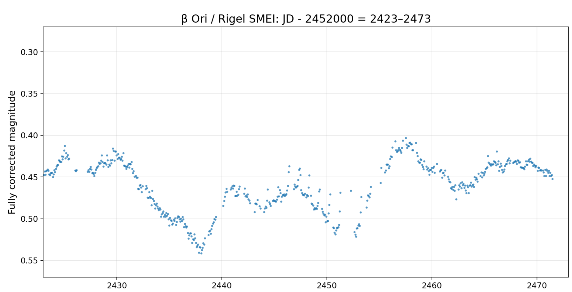

Figure 15: SMEI Rigel light curve for days 2423-2473 after JD 2452000.

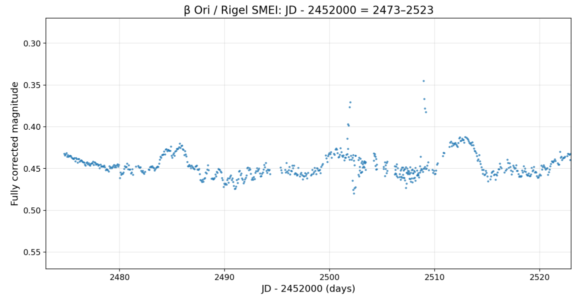

Figure 16: SMEI Rigel light curve for days 2473-2523 after JD 2452000.

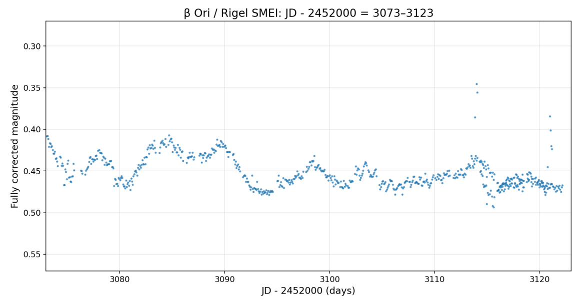

Figure 17: SMEI Rigel light curve for days 3073-3123 after JD 2452000.

Note that the periodogram for the full SMEI data set for Rigel (Figure 18) is of little help in quantifying or interpreting the behavior seen by inspection of the light curves. The short-period oscillations and the possible 5- or 10-day periodicities are less prominent in the periodogram compared to longer periods.

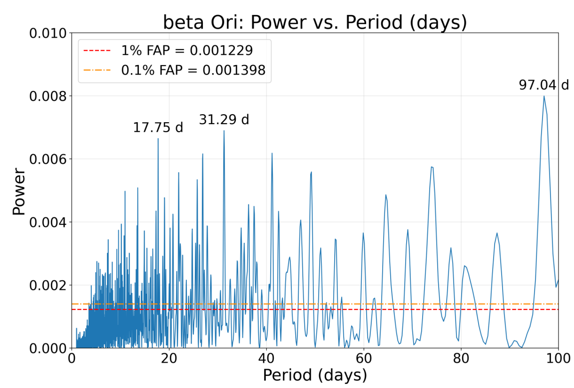

Figure 18: Lomb-Scargle periodogram generated from 8.6-year SMEI light curve for Rigel.

4.2 SMEI Comparison with MOST

An observing campaign for Rigel was conducted using the Canadian Microvariability and Oscillations of STars (MOST) satellite (Walker et al. 2003), with results presented by Moravveji et al. (2012a,b). The 27.7-day time span of the MOST observations from

Nov. 15 through Dec. 13, 2009, coincided with the time when SMEI was observing.

Figure 19 compares the MOST photometry from Moravveji et al. (2012a) with the SMEI fully corrected light curve at the same time. The agreement in the light curve shape is remarkable and goes a long way to validating the SMEI data. Moravveji et al. (2012a) attention to a portion of the light curve showing small-amplitude short-period oscillations such as we found in many segments of the Rigel SMEI data.

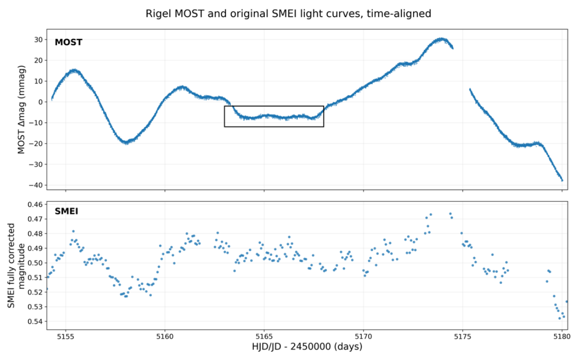

Figure 19: 27.7-day Rigel light curve from MOST spacecraft (top) compared with SMEI light curve (bottom). The square inset on the MOST data curve highlights a region where the stellar variability transitioned to low-amplitude short-period oscillations.

Moravveji et al. (2012a) also analyzed radial velocity measurements from spectra collected for 6.6 years by the 2-meter Tennessee State University Automatic Spectroscopic Telescope (Eaton and Williamson 2007) for 334 nights from December 11, 2003 through February 14, 2010. This entire time span was covered by SMEI data, and it will be interesting to determine whether there is a correlation between the radial velocity data and SMEI light curve.

Moravveji et al.'s (2012a) frequency analysis of the radial velocity data yielded 19 significant frequencies with periods between 1.2 and 74.7 days. Moravveji et al. (2012b) propose to explain these periods by nonradial gravity modes excited by the epsilon (ε) pulsation driving mechanism, but they can only explain periods longer than 21 days by this mechanism.

We did attempt to compare periods from Moravveji's list with the significant frequencies seen in the SMEI periodogram (Fig. 18). There are close matches in the SMEI data to all of the periods in the Moravveji et al. data for periods longer than 3.5 days, but this is likely coincidental since there is a dense spectrum of significant periods in the SMEI periodogram.

4.3 BRITE Constellation Light Curves

We also found that Rigel observations are available from the BRITE Constellation satellites (Weiss et al. 2014), available on the BRITE public data archive (https://brite.camk.edu.pl/pub/). The BRITE Constellation consists of five nanosatellites launched into low Earth orbit in 2013-2014, three observing in red and two in blue passbands. The satellites observed the target for 15-35 minutes per orbit, acquiring a photometric data point every 21 seconds, with 1 to 5-second exposures per observation. The BRITE data for Rigel were decorrelated by A. Pigulski.

We downloaded and plotted the data available from the five satellites for observing seasons in 2013, 2014, and 2015. Figure 20 shows the light curves colored by satellite for 2013-2014; the 2015 light curves were nearly featureless, so we have omitted them in this plot. It is interesting that one can see a large amplitude periodicity in the UBr data (orange) which could correlate with the approximate 75-day periodicity seen in the SMEI Rigel periodogram, and also with the longest-period significant periodicity in the Moravveji et al. (2012a) radial velocity data (74.7 days). Figure 21 zooms in on these data to better show the 75-day periodicity. Figure 22 zooms in on the time period between days 700 and 735 after BJD 2456000 for the 2013 BAb data (blue), showing oscillations of around 7 days, similar in period to the 7.18-day period in the Moravveji et al. (2012a) analysis and to some of the undulation periods seen in the SMEI Rigel light curves of Figs. 14-17.

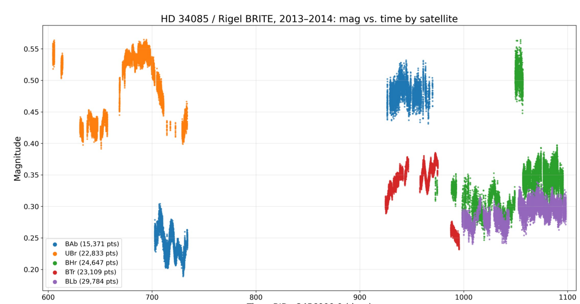

Figure 20: Rigel light curves from BRITE Constellation observations of 2013 and 2014.

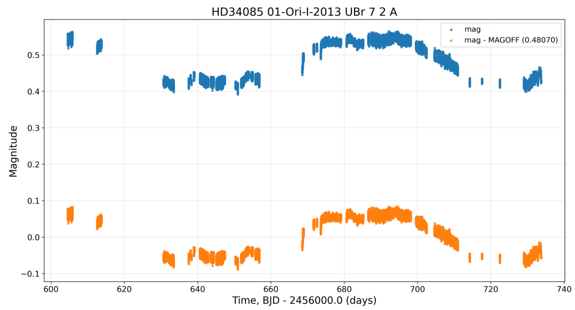

Figure 21: Zoom-in on UBr 2014 Rigel observations showing evidence of 75-day periodicity. The top blue curve is absolute magnitude; the bottom orange curve is offset by the average magnitude.

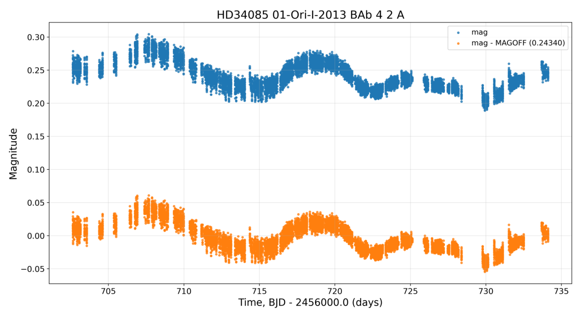

Figure 22: Zoom-in on BAb 2014 Rigel observations showing shorter-period variability. The top blue curve is absolute magnitude; the bottom orange curve is offset by the average magnitude.

4.4 AAVSO PEP Team Observations

The AAVSO PEP observing team has made a special effort to target Rigel for the past observing season. Figure 23 shows the light curve for November 2025 through March 2026, with observations taken by Michael Camilleri, Kevin Witman, and Paul Kneipp. The data set is a little sparse to confirm any periodicities but continued observing shows promise for finding long-term trends and perhaps confirming inferences or predictions made by closer examination of the SMEI Rigel light curve.

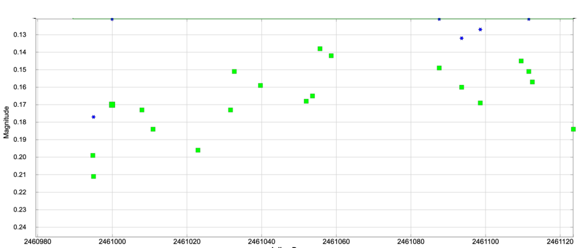

Figure 23: AAVSO PEP Rigel observations (green—V-band; blue—B-band) from November 2025 through March 2026.

5. Conclusions

To summarize some highlights from this investigation:

1. We extracted 8.6-year light curves from SMEI data for 33 of the 185 ACYG variables in the AAVSO VSX database. Lomb-Scargle periodograms of the full datasets usually show many significant low-frequency signals, similar to those seen in Stochastic Low-Frequency (SLF) variables (see, e.g., Pedersen and Bildsten 2025). Excepting V0566 Cas, the SMEI periodograms do not show strong peaks corresponding to the periods listed in VSX, when such periods are listed.
2. The SMEI light curves contain information that periodograms of the full data set do not capture. The SMEI light curve for Rigel (Guzik et al. 2025), and previous work on Deneb by Guzik et al. (2024), show transitions between intervals of larger-amplitude, longer-period variability and intervals of lower-amplitude or less coherent variability. In Rigel, we see small-amplitude, short-period oscillations punctuated by moderate-amplitude variations of about 0.05 magnitudes with periods near 5 days, as well as stretches of 0.1–0.2 magnitude variability with longer periods. It will be worthwhile to examine all 33 SMEI light curves in this way and quantify whether and how often transitions occur and how long they last.
3. The 27.7-day MOST light curve for Rigel agrees very well with the contemporaneous SMEI light curve. This comparison validates the SMEI light-curve reductions and supports using SMEI to study long-term variability in other bright ACYG stars.
4. We identify two possible gravity-mode/Rossby-mode pulsators: TIC 179508685, using 36 sectors of TESS data, and 19 Cep, using the 8.6-year SMEI data set. These two stars are excellent candidates for detailed asteroseismic studies.
5. This work reinforces the importance of long-term ground-based monitoring by amateur observers. Most ACYG stars have been observed by TESS, but the time series are usually short, not contiguous, and often complicated by contamination, saturation for bright stars, detrending that can remove real long-period variability, and difficulty stitching sectors together on the same absolute scale. Long-term ground-based observations can help quantify changes in variability patterns like those seen in Rigel and Deneb, especially when observers can keep uncertainties small.

Finally, we return to the question of whether ACYG variables are a homogeneous class. As an observational classification, the designation remains useful: these are luminous supergiants with low-amplitude variability, usually on timescales of days to weeks. However, the evidence does not support treating them as a homogeneous physical class. Some ACYG stars appear to be gravity-mode or Rossby-mode pulsators, and Moravveji et al. (2012b) found that the longer-period modes in Rigel could be explained by gravity-mode pulsations driven by the epsilon mechanism. Many of the SMEI periodograms resemble those of SLF variables, although the physical causes of SLF variability are debated. Later-type ACYG stars such as Deneb may have more in common with pulsating yellow supergiants than with OB-type SLF stars. Evolutionary state may also matter, since stars crossing the H-R diagram for the first time may not vary in the same way as stars returning blueward after a red-supergiant phase. We therefore conclude that ACYG variables listed in the VSX database are not a homogeneous physical class, but it is premature to divide them into physical subclasses based on variability mechanism or other properties.

6. Future Work

For future work, we have a long list of short-term and long-term projects:

1. Analyze the TESS data for the ACYG variables using reduction methods that preserve long-period variability and enable accurate absolute comparisons between data taken during different sectors.
2. Finish artifact removal for the SMEI ACYG light curves, document the reduction pipeline, and publish the processed light curves for the 33 bright ACYG variables examined here.
3. Extract significant frequencies and carry out stellar modeling for the candidate gravity-mode/Rossby-mode pulsators TIC 179508685 and 19 Cep.
4. Check whether *Kepler* (Borucki et al. 2010) or *K2* (Howell et al. 2014) observations are available for ACYG stars, and whether useful light curves can be extracted from full-frame images.
5. Compare the 6.6-year radial-velocity curve for Rigel discussed by Moravveji et al. (2012a) with the SMEI light curve from the same time period.
6. Examine halo photometry for the brightest ACYG stars. Rudrasingam et al. (2026) published several sectors of TESS halo photometry for Deneb, but Rigel was excluded because of its extreme brightness.
7. Continue ground-based monitoring of ACYG stars, including Deneb, Rigel, sigma Cyg, andV0566 Cas, and possibly additional stars such as Aludra. When TESS light curves are available at the same time, compare the space-based and ground-based observations directly. Because ACYG amplitudes are small, observers must continue to minimize and accurately estimate uncertainties in the ground-based data.
8. Place all ACYG variables more accurately on the Hertzsprung-Russell diagram to better constrain their evolutionary states.
9. Literature review and modeling of evolution and variability mechanisms for supergiants to determine whether the ACYG designation should eventually be divided into physically distinct subclasses.

7. Acknowledgements

This work makes use of data from NASA's Transiting Exoplanet Survey Satellite (TESS), obtained from the Mikulski Archive for Space Telescopes (MAST). Funding for the TESS mission is provided by NASA's Science Mission Directorate.

We acknowledge the use of open-source software including *astropy (astropy.org)* and *TESS Extractor (www.tessextractor.app)*.

This research has made use of the International Variable Star Index, VSX (vsx.aavso.org), operated by the AAVSO, Cambridge, Massachusetts, USA. This research also made use of data from the AAVSO International Database, and we thank the AAVSO observers Michael Camilleri, Kevin Witman, Paul Kneipp, Erwin van Bellegoij, David Brooks, Tom Calderwood, Brad Ferguson, Marcus Geselle, and Pam Morgan-McKee.

This work has made use of the SIMBAD database, operated at CDS, Strasbourg, France and of data from the European Space Agency mission Gaia, processed by the Gaia Data Processing and Analysis Consortium. Funding for the Gaia Data Processing and Analysis Consortium has been provided by national institutions, in particular, the institutions participating in the Gaia Multilateral Agreement.

Based on data collected by the BRITE Constellation satellite mission, designed, built, launched, operated and supported by the Austrian Research Promotion Agency, the University of Vienna, the Technical University of Graz, the University of Innsbruck, the Canadian Space Agency, the University of Toronto Institute for Aerospace Studies, the Foundation for Polish Science & Technology, and the National Science Centre. We thank A. Pigulski for decorrelating the BRITE Rigel data.

We acknowledge support from Los Alamos National Laboratory, managed by Triad National Security, LLC, for the U.S. Department of Energy's National Nuclear Security Administration under Contract No. 89233218CNA000001.

Portions of the manuscript preparation, language editing, and figure/data-analysis were assisted by ChatGPT 5.5 and Claude Sonnet; scientific interpretations and final text were reviewed by the authors.

8. References

Abt, H.A., Guzik, J.A., and Jackiewicz, J. 2023, The Abrupt Resumptions of Pulsations in α Cygni (Deneb), PASP 135, **1054**, 124201

Allen's Astrophysical Quantities, Fourth Edition, ed. Arthur N. Cox, Springer: AIP Press, 2000, pp. 388-389

Astropy Collaboration. 2022, The Astropy Project: Sustaining and Growing a Community-oriented Open-source Project and the Latest Major Release (v5.0) of the Core Package, ApJ **935**, 167

Bódi, A. and Kiss, L.L. 2019, Physical Properties of Galactic RV Tauri Stars from Gaia DR2 Data, ApJ **872**, 60, doi: 10.3847/1538-4357/aafc24

Borucki, W.J., et al. 2010, *Kepler* Planet-Detection Mission: Introduction and First Results, Science **327**, 5968, doi: 10.1126/science.1185402

Clover, J.M., et al. 2011, Epsilon Aurigae light curve from the Solar Mass Ejection Imager, AAS Meeting Abstracts **217**, 257.02

Eaton, J.A. and Williamson, M.H. 2007, The Tennessee State University Automatic Spectroscopic Telescope: Data Processing and Velocity Variation of Cool Giants, **PASP** 119, 886

Gaia Collaboration, Gaia Data Release 3, 2023, Summary of the content and survey properties, A&A **674**, A1

Guzik, J.A., Abt, H., Jackiewicz, J., and Kloppenborg, B.K. 2024a, Abrupt Periodic Pulsation Resumptions in Deneb, Proceedings of the 112th Annual Meeting of the AAVSO, https://www.aavso.org/112, doi: 10.48550/arXiv.2410.23936

Guzik, J.A., Kloppenborg, B., and Jackiewicz, J. 2024b, Deneb and the Alpha Cygni Variables, Society for Astronomical Sciences Symposium on Telescope Sciences 2024 proceedings, eds. J.C. Martin, R.K. Buchheim, R.M. Gill, W. Green, and J. Menke, https://socastrosci.org/wp-content/uploads/2024/08/2024-Proceedings_Ver1.3d.pdf, arXiv.2410.23985

Guzik, J.A., Kloppenborg, B., Richardson, N., Jackiewicz, J., Morrison, N., Calderwood, T., and Pigulski, A. 2025, Abrupt Pulsation Resumptions in Deneb: An Update, Proceedings of the 113th Annual Meeting of the American Association of Variable Star Observers, Huntsville, AL, Nov. 8-10, 2024, www.aavso.org/113, arXiv:2503.20058

Guzik, J.A., Whitley, C., Moore, N., Marshall, M., and Jackiewicz, J. 2026, Alpha Cygni Variables as Seen from the Transiting Exoplanet Survey Satellite, Proceedings of the 114th Annual Meeting of the American Association of Variable Star Observers, Portland, OR, Nov. 1-2, 2025, www.aavso.org/114, arXiv:2603.02421

Howell, S.B., et al. 2014, The K2 mission: Characterization and early results, PASP **136**, 398

Humphreys, R.A. and Davidson, K. 1994, The Luminous Blue Variables: Astrophysical Geysers, PASP **106**, 1025

Jackson, B.V., et al. 2004, The Solar Mass Ejection Imager (SMEI) Mission, Sol. Phys. **225**, 177

Jeffery, C.S. 2025, Linear and non-linear models for large-amplitude radial pulsation in faint blue stars (BLAPs), MNRAS **538**, issue 4, 2952-2988, https://doi.org/10.1093/mnras/staf401

Kloppenborg, B.K. 2023, Observations from the AAVSO International Database, https://www.aavso.org

Li, G., et al. 2019, Period spacings of γ Doradus pulsators in the Kepler field: Rossby and gravity modes in 82 stars, MNRAS **487**, 782

Moravveji, E., Guinan, E.F., Shultz, M., Williamson, M.H., and Moya, A. 2012a, Asteroseismology of the nearby SN-II progenitor: Rigel. I. The MOST high-precision photometry and radial velocity monitoring, ApJ **747**, 108

Moravveji, E., Moya, A., and Guinan, E.F. 2012b, Asteroseismology of the nearby SN II progenitor Rigel. II. ε-mechanism triggering gravity-mode pulsations? ApJ **749**, 74

Pedersen, M.G. and Bildsten, L. 2025, Stochastic low-frequency variability of 50 massive stars in the Cygnus

OB associations and the Small Magellanic Cloud, MNRAS **539**, 2742

Richardson, N.D., et al. 2011, A Five-Year Spectroscopic and Photometric Campaign on the Prototypical a Cygni Variable and A-Type Supergiant Star Deneb, AJ **141**, 17, doi:10.1088/0004-6256/141/1/17

Ricker, G.R., et al. 2015, Transiting Exoplanet Survey Satellite, Journal of Astronomical Telescopes, Instruments, and Systems, Volume 1, id. 014003

Rudrasingam, J., et al. 2026, Halo photometry and asteroseismology for 98 of the brightest stars observed by TESS, MNRAS **547**, 1

Saio, H., et al. 2018, Theory and evidence of global Rossby waves in upper main-sequence stars: r-mode oscillations in many *Kepler* stars MNRAS **474**, 2774

Serna, J., et al. 2021, Stellar Rotation of T Tauri Stars in the Orion Star-forming Complex, ApJ **923**, 177, doi: 10.3847/1538-4357/ac300a

Stankov, A. and Handler, G. 2005, Catalog of Galactic β Cephei Stars, ApJSS **158**, 193, doi: 10.1086/429408

Stassun, K., et al. 2019, The Revised TESS Input Catalog and Candidate Target List, AJ **158**, 138, doi: 10.3847/1538-3881/ab3467

van Genderen, A., et al. 1989, Light variations of massive stars (alpha Cygni variables). IX., A&AS **79**, 263

Walker, G., et al. 2003, The MOST Asteroseismology Mission: Ultraprecise Photometry from Space, PASP **115**, 1023

Watson, C.L., Henden, A.A., and Price, A. 2006, The International Variable Star Index (VSX), Society for Astronomical Sciences Annual Symposium, Vol. 25, 47

Weiss, W.W., et al. 2014, BRITE-Constellation: Nanosatellites for Precision Photometry of Bright Stars, PASP **126**, 57.